

Optical studies of charge dynamics in c -axis oriented superconducting MgB₂ films

J.J. Tu,^{1,*} G.L. Carr,² V. Perebeinos,¹ C.C. Homes,¹ M. Strongin,¹ P.B. Allen,³ W.N. Kang,⁴ Eun-Mi Choi,⁴
Hyeong-Jin Kim,⁴ and Sung-Ik Lee⁴

¹*Department of Physics, Brookhaven National Laboratory, Upton, New York 11973-5000*

²*NSLS, Brookhaven National Laboratory, Upton, New York 11973-5000*

³*Department of Physics and Astronomy, SUNY Stony Brook, Stony Brook NY 11794-3800*

⁴*National Creative Research Initiative Center for Superconductivity, Department of Physics, Pohang University of Science and Technology, Pohang 790-784, Korea*

(November 11, 2018)

Temperature dependent optical conductivities and DC resistivity of c -axis oriented superconducting ($T_c = 39.6$ K) MgB₂ films (~ 450 nm) have been measured. The normal state ab -plane optical conductivities can be described by the Drude model with a temperature independent Drude plasma frequency of $\omega_{p,D} = 13\,600 \pm 100$ cm⁻¹ or 1.68 ± 0.01 eV. The normal state resistivity is fitted by the Bloch-Grüneisen formula with an electron-phonon coupling constant $\lambda_{tr} = 0.13 \pm 0.02$. The optical conductivity spectra below T_c of these films suggest that MgB₂ is a multi-gap superconductor.

PACS: 74.25.Gz, 74.76.Db, 74.25.Kc

The recent discovery of superconductivity in MgB₂ with T_c of 39 K has generated much scientific interest [1]. As in the case of the high- T_c cuprates, debate rages as to the mechanism of superconductivity in this material. Initial isotope effect measurements suggested electron-phonon coupling as the pairing mechanism for superconductivity in MgB₂ [2,3]. Many theoretical studies [4–7] since then have concluded that strong electron-phonon coupling is responsible for the high transition temperature, with $\lambda \sim 1$. However, other pairing mechanisms have also been proposed, e.g. ‘dressing’ and ‘undressing’ of holes [8], acoustic plasmons [9] and the ‘filamentary’ theory [10]. This inconclusive state of affairs is mainly due to the lack of consensus on many important physical quantities in MgB₂. For example, the reported values for the superconducting gap 2Δ vary from 4 meV [11] to 15 meV [12]. Infrared spectroscopy is able to measure such quantities as the scattering rate $1/\tau$, the Drude plasma frequency $\omega_{p,D}$ and 2Δ [13]. In this work, we analyze the optical data of MgB₂ to determine the electron-phonon coupling constant, λ_{tr} , in a similar fashion as in the optical study [14] of Ba_{0.6}K_{0.4}BiO₃ ($T_c \sim 30$ K), where $\lambda_{tr} \sim 0.2$ was obtained experimentally.

There have been very few optical studies on MgB₂ to date. Gorshonov *et al.* [15] measured the reflectance of a polycrystalline pellet using the grazing angle method and set a lower limit of 2Δ to be 3–4 meV. Pronin *et al.* [16] examined the complex optical conductivity of a MgB₂ thin film in the frequency range of 0.5–4 meV. More recently, Jung *et al.* [17] carried out transmission measurements on a c -axis oriented MgB₂ film (~ 50 nm) with $T_c \sim 33$ K and fitted the data with a gap value of $2\Delta(0) \sim 5.2$ meV. However, to obtain the optical constants of bulk MgB₂ in a wide frequency region, reflectivity measurements are the preferred method.

In this Letter, temperature dependent optical conductivities and DC resistivity of c -axis oriented superconducting ($T_c = 39.6$ K) MgB₂ films (~ 450 nm) are re-

ported. The normal state ab -plane optical conductivities can be well described by the Drude model with $\omega_{p,D} = 13600 \pm 100$ cm⁻¹. Using this plasma frequency $\lambda_{tr} = 0.13 \pm 0.02$ is determined by fitting the DC resistivity data. In addition, the optical conductivities in the superconducting state exhibit complex behavior suggesting that MgB₂ is a multi-gap superconductor.

For this study, several c -axis oriented MgB₂ films are used: one very thin film (~ 50 nm) similar to the film studied by Jung *et al.* [17] and two thicker films (~ 450 nm). These high-quality c -axis oriented films were deposited on c -cut Al₂O₃ substrates using a pulsed laser deposition method as described previously [18]. X-ray measurements showed that the MgB₂ grains were highly oriented with their c -axes normal to the substrate. These MgB₂ films have a tan appearance, similar to the high purity MgB₂ polycrystalline samples [2]. The thick MgB₂ films (~ 450 nm) are opaque in the visible region.

The Al₂O₃ substrates with the MgB₂ films are mounted on an optically-black cone, and the temperature dependent reflectance is measured in a near-normal-incidence arrangement from ~ 30 to over $22\,000$ cm⁻¹, with the electric field parallel to the ab -plane on Bruker IFS 66v/S and 113v spectrometers. The absolute reflectance is determined by evaporating a gold film *in situ* in ultra-high vacuum ($\sim 10^{-8}$ Torr). The details of this technique have been described previously [19]. The optical conductivities are then determined from a Kramers-Kronig analysis of the reflectance.

In Fig. 1(a), the temperature dependent DC sheet resistance, R_{\square} , measured by a standard four-probe technique of a MgB₂ film (~ 450 nm) is shown. The residual resistance ratio (RRR) of R_{\square} at 295 K and at 40 K is 2.2. The low temperature region near T_c is given in the insert of Fig. 1(a). The superconducting transition in this film is extremely sharp with a transition region of $\delta T_c < 0.1$ K and a T_c of 39.6 K indicating that these

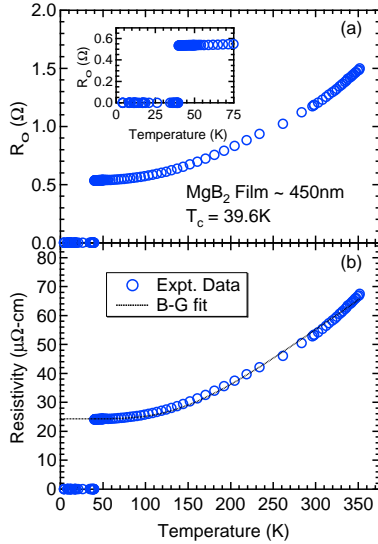


FIG. 1. The DC resistivity data of a *c*-axis oriented MgB₂ film (*t* ~ 450 nm). (a) Temperature dependent R_{\square} (open circles). Inset: low temperature region of R_{\square} near T_c ; (b) Temperature dependence of the resistivity together with a fit to the Bloch-Grüneisen formula.

thick MgB₂ films are of excellent quality [18].

The raw data of the optical measurements on these MgB₂ films (~ 450 nm) are summarized in Fig. 2. The absolute reflectance is quite high as shown in Fig. 2(a), however, several sharp phonon features can be clearly identified. As a comparison, the reflectance of the thin MgB₂ film (~ 50 nm) is also measured. The two strong infrared active TO-phonons of *c*-cut Al₂O₃ crystals at 440 and 570 cm⁻¹ [20] can be easily observed for the thin MgB₂ film but completely absent in the reflectance data of the thick films (~ 450 nm), indicating that the thick films are totally opaque. Therefore, the *ab*-plane optical properties measured for these MgB₂ films (~ 450 nm) are intrinsic. In the insert, the reflectance data at 295 K is given for the entire frequency region: from 30 to 22000 cm⁻¹. The largest possible frequency interval is needed to carry out a reliable Kramers-Kronig analysis. The results of such an analysis are shown as temperature dependent $\sigma_1(\omega)$ in Fig. 2(b) and $\sigma_2(\omega)$ in Fig. 2(c). Superconducting behavior can be easily identified as a drop in $\sigma_1(\omega)$ at low frequencies below T_c .

The normal state optical conductivities of these MgB₂ films are analyzed in Fig. 3. In Fig. 3(a), $\sigma_1(\omega)$ and $\sigma_2(\omega)$ at 295 K are shown. Both the real and imaginary parts of the optical conductivities at low frequencies can be well described by the simple Drude model of the form:

$$\bar{\sigma}(\omega) = \sigma_1 + i\sigma_2 = \frac{1}{4\pi} \frac{\omega_{p,D}^2 \tau}{1 - i\omega\tau}, \quad \omega_{p,D}^2 = \frac{4\pi n e^2}{m^*} \quad (1)$$

where $\omega_{p,D}$ is the Drude plasma frequency, $1/\tau$ is the scattering rate, n is the number of free-carriers per unit volume and m^* is the average effective mass of the occupied carrier states. The Drude model describes the

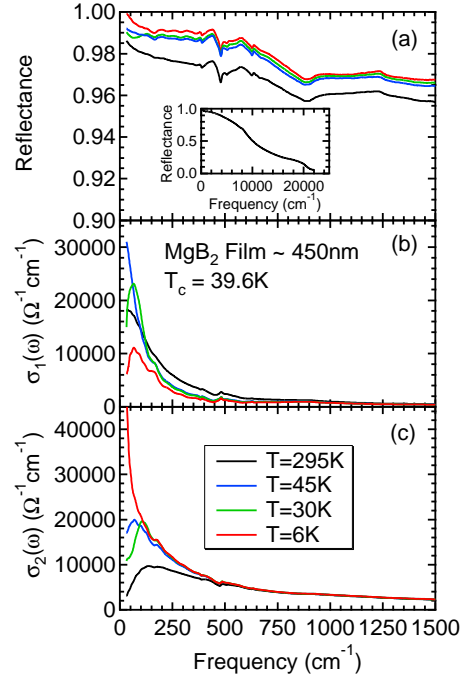


FIG. 2. The temperature dependent *ab*-plane optical data of *c*-axis oriented MgB₂ films (*t* ~ 450 nm) from 30 to 1500 cm⁻¹. (a) The reflectance data showing sharp phonon modes. Inset: optical reflectance spectrum for the entire frequency region at 295 K; (b) Temperature dependent $\sigma_1(\omega)$; (c) Temperature dependent $\sigma_2(\omega)$.

experimental data surprisingly well at 295 K. The fitting parameters have the values $\omega_{p,D} = 13600 \pm 100$ cm⁻¹, and $1/\tau = 170 \pm 5$ cm⁻¹. This Drude plasma frequency of 13600 cm⁻¹ is quite consistent with the value obtained from an optical study of a polycrystalline MgB₂ sample [21]. However, in addition to the Drude peak, some other contributions to $\sigma_1(\omega)$ are also observed in that optical study [21]. Using the optical data, one can determine the DC resistivity $\rho = 1/\sigma_0$ to be 53 ± 2 μΩ-cm at 295 K. Thus, the averaged thickness of this MgB₂ film is derived as $t = \rho/R_{\square} = 450 \pm 20$ nm which agrees very well with the typical thickness of 400 nm of these films [18]. The DC resistivity can now be plotted as shown in Fig. 1(b). It is interesting that the experimental Drude plasma frequency of 1.68 eV is much smaller than the value of ~ 7 eV predicted by calculations of the electronic structure in MgB₂ [4–7]. These calculations usually give values of Drude plasma frequencies that are reasonably close to experimental values, even in highly correlated systems like high T_c cuprates [22].

Keeping $\omega_{p,D}$ the same, the optical conductivities at 45 K are fitted with Eq. (1). The results are given in Fig. 3(b). Both $\sigma_1(\omega)$ and $\sigma_2(\omega)$ again fit well with the Drude model with a scattering rate of $1/\tau = 75 \pm 5$ cm⁻¹. In addition, the DC resistivity at 45 K is in good agreement with the zero frequency extrapolation of $\sigma_1(\omega)$. Therefore, the DC conductivity and real part the optical

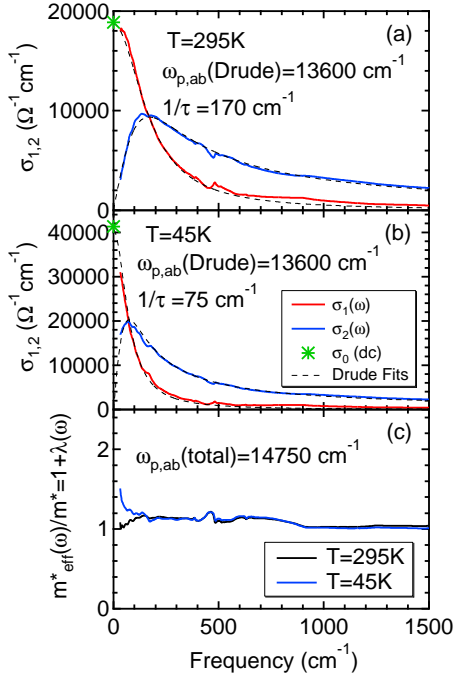


FIG. 3. The analysis of normal state *ab*-plane optical constants of the *c*-axis oriented MgB₂ films. (a) Frequency dependent optical conductivities: $\sigma_1(\omega)$ and $\sigma_2(\omega)$ at 295 K with the Drude fits; (b) Frequency dependent optical conductivities at 45 K; (c) Frequency dependent effective mass ratio for $T > T_c$.

conductivity are in excellent agreement.

From the *ab*-plane optical data, one can calculate the frequency dependent electron-phonon coupling constant $\lambda(\omega)$ in the extended Drude formalism [23]:

$$\frac{m^*_{\text{eff}}(\omega)}{m^*} = 1 + \lambda(\omega) = \frac{1}{4\pi} \frac{\omega_p^2}{\omega} \text{Im} \left[\frac{1}{\tilde{\sigma}(\omega)} \right], \quad (2)$$

where ω_p is the total plasma frequency of free *ab*-plane carriers. The purpose of casting the optical data in the extended Drude form is to account for the small deviations from the simple Drude model by using a frequency dependent scattering rate $1/\tau(\omega)$. The result of this analysis is shown in Fig. 3(c). The value of $\lambda(\omega)$ derived optically varies from 0 to about 0.2 in the optical phonon region, where $\omega_p = 14750 \pm 150\text{ cm}^{-1}$ is derived from the conductivity sum rule. The value of ω_p is slightly larger than $\omega_{p,D}$ due to the fact that the sum rule captures additional spectral weight in the high frequency region.

The electron-phonon coupling constant λ_{tr} is traditionally determined from the temperature dependent DC resistivity using the Bloch-Grüneisen formula

$$\rho(T) = \rho_0 + \lambda_{tr} \frac{4\pi}{\omega_{p,D}^2} \frac{128\pi(k_B T)^5}{(k_B \Theta_D)^4} \int_0^{\frac{\Theta_D}{2T}} \frac{x^5}{\sinh^2 x} dx, \quad (3)$$

with three parameters: ρ_0 - the residual resistivity at $T = 0$; Θ_D - the Debye temperature and λ_{tr} . A non-linear least squares fit to the resistivity data with the

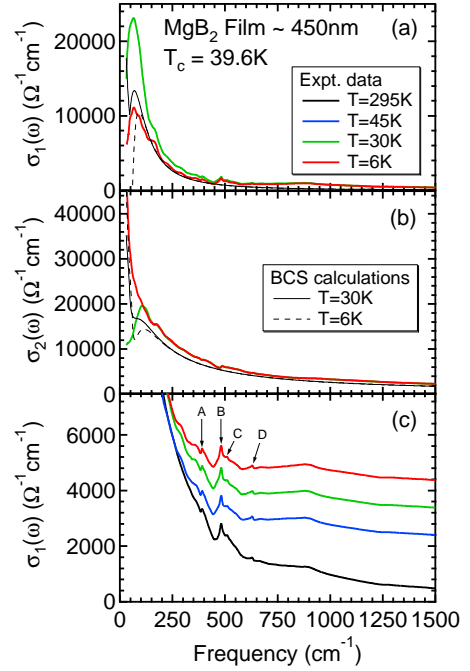


FIG. 4. The analysis of superconducting state *ab*-plane optical constants of the *c*-axis MgB₂ films. (a) Temperature dependent $\sigma_1(\omega)$ (thick lines) with the BCS fits; (b) Temperature dependent $\sigma_2(\omega)$ with the BCS fits; (c) Temperature dependent $\sigma_1(\omega)$ showing four Γ -point phonons. The spectra corresponding to different temperatures are offset for clarity.

Eq. (3) is given in Fig. 1(b) using $\omega_{p,D} = 1.68 \pm 0.01\text{ eV}$. The experimental curve and the theoretical fit agree quite well with the fitting parameters: $\rho_0 = 24.3 \pm 0.3\ \mu\Omega\text{-cm}$; $\Theta_D = 950 \pm 100\text{ K}$ and $\lambda_{tr} = 0.13 \pm 0.02$. The value $\Theta_D = 950 \pm 100\text{ K}$ is consistent with the experimentally measured value that varies from 800 K [24] to 1050 K [25]. However, $\lambda_{tr} = 0.13 \pm 0.02$ is significantly smaller than most theoretical predictions of $\lambda \sim 1$ [4–7] in MgB₂.

The optical conductivities of these MgB₂ films in the superconducting state are examined in Fig. 4. The superfluid plasma frequency is found to be $\omega_{p,S} = 7300 \pm 50\text{ cm}^{-1}$ at 6 K from the Ferrel-Glover-Tinkham sum rule. However, the optical spectra below T_c cannot be fitted by the BCS model using a single isotropic gap. Theoretical curves at 30 K and 6 K generated with a BCS model [26] are shown in Figs. 4(a) and 4(b). The parameters used are: $2\Delta = 65\text{ cm}^{-1}$ and $1/\tau = 75\text{ cm}^{-1}$. There are significant deviations between the experimental data and the BCS calculations. However, from our optical data the upper and lower limits of the superconducting gap can be estimated: $5\text{ meV} < 2\Delta_x < 15\text{ meV}$. The complex gap behavior observed in our optical conductivity data in the superconducting state adds support to the suggestion that MgB₂ is a multi-gap superconductor [5,12,25].

Four sharp phonon peaks can be identified in $\sigma_1(\omega)$ as shown in Fig. 4(c) that can be assigned to Γ -point optical phonons in MgB₂ [4]. The two strong phonon

peaks marked as A and B are the two infrared active lattice modes: at 380 cm^{-1} (E_{1u}) and at 480 cm^{-1} (A_{2u}). Their relatively large oscillator strengths are the consequence of the low plasma frequency in MgB_2 . Two weak phonon peaks marked as C and D at 510 cm^{-1} and 630 cm^{-1} are tentatively assigned as the Raman active E_{2g} mode and the silent B_{1g} mode according to the phonon calculations [4]. These two phonons with even symmetry become infrared active because of the lattice imperfections in the films. Alternatively, several Raman studies [27] on MgB_2 have assigned a very broad band centered at 620 cm^{-1} as the E_{2g} mode. In addition, three broad features are also observed at 160, 880 and 1240 cm^{-1} in $\sigma_1(\omega)$. The resolution of this optical study is 4 cm^{-1} in the phonon region, and none of the four sharp phonon modes exhibit detectable changes in either their intensities, peak positions, or line-widths going through T_c .

The surprising aspect of our results is the small value of $\lambda_{tr} = 0.13$ derived from both the DC resistivity and optical conductivity measurements. A simple application of McMillan formula [28] with $\lambda \cong \lambda_{tr} = 0.13$ will give $T_c < 1\text{ K}$. However, there are several reasons why the BCS theory should not be abandoned right way for MgB_2 : 1) the superconducting gap in MgB_2 has unusual properties. Gap anisotropy including dimensional effects [29] modifies T_c relative to the McMillan formula; 2) the λ value that goes into the McMillan formula can differ somewhat with respect to λ_{tr} [30]; 3) *c*-axis optical and transport properties should be experimentally studied. On the other hand, given the small value of $\lambda_{tr} = 0.13$ alternative mechanisms of superconductivity in MgB_2 should be examined both experimentally and theoretically. It is interesting to note that many of the optical constants in MgB_2 are quite similar to those in $\text{Ba}_{0.6}\text{K}_{0.4}\text{BiO}_3$ [14], e.g. the scattering rate, the Drude plasma frequency, and particularly the small value of λ_{tr} . A common mechanism might be responsible for superconductivity in both systems. In addition, having a small free-carrier plasma frequency ($< 3\text{ eV}$) seems to be an universal characteristic shared by almost all superconductors with a $T_c > 30\text{ K}$.

In conclusion, we have measured optical conductivities and DC resistivity of *c*-axis oriented superconducting MgB_2 films. With a Drude plasma frequency of $\omega_{p,D} = 13600 \pm 100\text{ cm}^{-1}$, $\lambda_{tr} = 0.13 \pm 0.02$ is determined from DC resistivity data. The small measured λ_{tr} value poses a serious problem to the strong electron-phonon coupling picture. Other theoretical models need to be explored to account both for the complex behavior of the superconducting gap and possible different pairing mechanism in MgB_2 .

We thank P.C. Canfield, V.J. Emery, J.E.Hirsch, P.D. Johnson, S.A. Kivelson, G. Schneider, T. Valla, T. Vogt, and Z. Yusof for helpful discussions. Part of the work was supported by the U.S. Department of Energy under Contract No. DE-AC02-98CH10886 and the other

part by the Ministry of Science and Technology of Korea through the Creative Research Initiative Program. Research undertaken at NSLS was supported by the U.S. DOE, Division of Materials and Chemical Sciences.

* Electronic address: jtu@bnl.gov

- [1] J. Nagamatsu *et al.*, Nature (London) **410**, 63 (2001).
- [2] S.L. Bud'ko *et al.*, Phys. Rev. Lett. **86**, 1877 (2001).
- [3] D.G. Hinks, H. Claus, and J.D. Jorgensen, cond-mat/0104242.
- [4] J. Kortus *et al.*, Phys. Rev. Lett. **86**, 4656 (2001).
- [5] A.Y. Liu, I.I. Mazin, and J. Kortus, cond-mat/0103570.
- [6] Y. Kong, O.V. Dolgov, O. Jepsen, and O.K. Anderson, Phys. Rev. B **64**, 020501(R) (2001).
- [7] J.M. An and W.E. Pickett, Phys. Rev. Lett. **86**, 4366 (2001).
- [8] J.E. Hirsh and F. Marsiglio, cond-mat/0102479.
- [9] K. Voelker, V.I. Anisimov, and T.M. Rice, cond-mat/0103082.
- [10] J.C. Phillips and J. Jung, cond-mat/0102261.
- [11] G. Rubio-Bollinger, H. Suderow, and S. Vieira, Phys. Rev. Lett. **86**, 5582 (2001).
- [12] F. Giubileo *et al.*, cond-mat/01045146.
- [13] M. Tinkham, *Introduction to Superconductivity* (Krieger, Malabar, 1975); B. Farnworth and T. Timusk, Phys. Rev. B **10**, 5119 (1976); F. Gao *et al.*, Phys. Rev. B **54**, 700 (1996).
- [14] A.V. Puchkov, T. Timusk, W.D. Mosley, and R.N. Shelton, Phys. Rev. B **50**, 4144 (1994).
- [15] B. Gorshunov *et al.*, cond-mat/0103164.
- [16] A.V. Pronin, A. Pimenov, A. Loidl, and S.I. Kransnosvobodtsev, cond-mat/0104291.
- [17] J.H. Jung *et al.*, cond-mat/0105180.
- [18] W.N. Kang *et al.*, Science **292**, 1521 (2001).
- [19] C.C. Homes, M. Reedyk, D. Crandles, and T. Timusk, Appl. Opt. **32**, 2972 (1993).
- [20] A.S. Barker, Phys. Rev. **132**, 1474 (1963).
- [21] A. B. Kuz'menko *et al.*, in *Sixth International Conference on Spectroscopy of Novel Superconductors*, edited by A. Bansil (Elsevier, Chicago, 2001), p. 51 (poster P28).
- [22] W.E. Pickett, P.B. Allen, and H. Krakauer, Phys. Rev. B **37**, 7482 (1988).
- [23] A.V. Puchkov, D.N. Basov, and T. Timusk, J. Phys. C **8**, 10 049 (1996).
- [24] R.K. Kremer, B.J. Gibson, and K. Ahn, cond-mat/0102432.
- [25] F. Bouquet *et al.*, cond-mat/0104206.
- [26] W. Zimmermann *et al.*, Physica C **183**, 99 (1991).
- [27] X. K. Chen *et al.*, cond-mat/0104005; A.F. Goncharov *et al.*, cond-mat/0104042; J. Hlinka *et al.*, cond-mat/0105275.
- [28] W.L. McMillan, Phys. Rev. **167**, 331 (1968); P.B. Allen and R.C. Dynes, Phys. Rev. B **12**, 905 (1975).
- [29] P.B. Allen, Z. Phys. B **47**, 45 (1982) (and references therein).
- [30] P.B. Allen, in *Handbook of Superconductivity*, edited by C.P. Poole (Academic, San Diego, 2000), p. 478.